Published in final edited form as:
Nat Neurosci. 2009 March ; 12(3): 311–317. doi:10.1038/nn.2275.

Non-cell autonomous influence of MeCP2-deficient glia on neuronal dendritic morphology

Nurit Ballas[1,3], **Daniel T. Lioy**[2,*], **Christopher Grunseich**[1,*], and **Gail Mandel**[1,2]

[1] Howard Hughes Medical Institute, Department of Neurobiology and Behavior, State University of New York, Stony Brook, New York, 11794

[2] Vollum Institute and Howard Hughes Medical Institute, Oregon Health and Science University, Portland, Oregon 97239

[3] Department of Biochemistry and Cell Biology, State University of New York, Stony Brook, New York, 11794-5215

Abstract

The neurodevelopmental disorder Rett Syndrome (RTT) is caused by sporadic mutations in the transcriptional factor methyl-CpG binding protein 2 (MeCP2). Although it is thought that the primary cause of RTT is cell autonomous due to lack of functional MeCP2 in neurons, whether non-cell autonomous factors contribute to the disease, is unknown. Here, we show that loss of MeCP2 occurs not only in neurons but also in glial cells of RTT brain. Using an *in vitro* co-culture system, we find that mutant astrocytes from a RTT mouse model, and their conditioned medium, fail to support normal dendritic morphology of either wild-type or mutant hippocampal neurons. Our studies suggest that in RTT brain, astrocytes carrying MeCP2 mutations have a non-cell autonomous effect on neuronal properties, likely due to aberrant secretion of soluble factor(s).

Rett Syndrome (RTT) is a neurodevelopmental disorder caused by sporadic mutations in the X-linked gene encoding *methyl-CpG binding protein 2* (*MeCP2*) [1]. Girls born with RTT attain normal developmental milestones for 6–18 months, after which they begin to regress, losing speech, motor skills, and purposeful hand motions. They also suffer myriad other problems including microcephaly, mental retardation, autism, severe respiratory distress, epileptic seizures, and overall retarded growth [2]. MeCP2 mutations in boys usually lead to neonatal encephalopathy and death during the first year of life.

MeCP2 is a member of the methyl-CpG-binding protein family that functions as transcriptional repressors and contains three functional domains: the methyl-DNA binding domain (MBD) that binds to methylated CpG dinucleotides, a transcriptional repressor domain (TRD) that can recruit corepressors and chromatin remodeling complexes, and the C-terminal domain that facilitates binding to DNA [3–5]. Repression is mediated, at least in some circumstances, by recruitment of the corepressors mSin3A and histone deacetylases (HDACs) [6,7]. MeCP2 also enhances histone H3 lysine 9 methylation, a modification associated with gene silencing [8]. MeCP2 is highly expressed in mature neurons and regulates activity-dependent gene expression [9,10] by a mechanism involving calcium-dependent phosphorylation of MeCP2 [11]. Further, MeCP2 is associated with

Correspondence should be addressed to N.B. (nballas@notes.cc.sunysb.edu).
*These two authors contributed equally to this work

Author Contributions. N.B., D.T.L., C.G, and G.M. designed the experiments. N.B., D.T.L., and C.G. carried out the experiments. N.B., D.T.L., and G.M. wrote the paper. N.B. and G.M. supervised the project.

transcriptionally active genomic regions [12,13] and may also regulate RNA splicing [14], suggesting that complex MeCP2 functions play a role in RTT pathogenesis.

There are several RTT mouse models, each of which contain different mutations in MeCP2 [15–17]. These models recapitulate many characteristic features of RTT, including a normal early developmental period followed by neurological dysfunction and early mortality. Importantly, conditional knockout specific to neural stem/progenitor cells, driven by the nestin-Cre transgene, results in a phenotype similar to the ubiquitous knockout [15,16], suggesting that MeCP2 dysfunction in the brain underlies RTT. Furthermore, conditional knockout of MeCP2 in post-mitotic neurons driven by the calcium-calmodulin-dependent protein kinas ll (CaMKll)-Cre transgene results in similar, although a significantly milder neurological phenotype [15,18], indicating an important role for MeCP2 in mature neurons. More recent studies indicate that mice born with RTT can be rescued by reactivation of normal MeCP2 expression [19,20], suggesting that the damage that occurs to neurons can be reversed. In addition to the genetic studies, the impact of MeCP2 dysfunction on neuronal structure and function in RTT patients and mice is further supported by several studies showing abnormalities in dendritic arborization [21,22], spine density [23], basal synaptic transmission [24], excitatory synaptic plasticity [24–26], and reduced spontaneous cortical activity [27].

Although these studies clearly suggest a neuropathology in RTT, whether the pathology is due exclusively to the lack of functional MeCP2 in neurons was not determined experimentally. Here, we show that MeCP2 is present in normal brain not only in neurons, but also in all types of glia, including astrocytes, oligodendrocyte progenitor cells (OPCs), and oligodendrocytes. While MeCP2 is clearly expressed in wild-type astrocytes, MeCP2 is absent in astrocytes of RTT mouse brains. Using a co-culture system based on two genetically distinct mouse models of RTT, we show that MeCP2-null astrocytes are unable to support normal neuronal growth. Furthermore, conditioned media from the MeCP2-null astrocytes phenocopies the astrocytic effect, suggesting that aberrantly secreted factors by the mutant astrocytes cause the neuronal damage. Importantly, hippocampal neurons in these cultures showed dendritic abnormalities observed in RTT patients and RTT mouse models. These findings indicate that MeCP2 dysfunction in glia likely plays a role in RTT neuropathology.

Results

MeCP2 is present in neurons and glia of normal brains

Several previous studies support the notion that, in the nervous system, MeCP2 is present exclusively in neurons, based on immunohistochemical analyses indicating that MeCP2 is highly expressed in neurons and undetectable in glia [17,21,28]. However, because MeCP2 is expressed in many different non-neuronal cell types outside of the nervous system, we sought to examine, more systematically, whether MeCP2 is expressed in glia, which represent a large non-neuronal cell population in the brain, and provide structural and functional support to neurons. Initially, we asked whether MeCP2 is present in enriched primary cultures of different types of wild-type glia from post-natal brain. Using an antibody directed to the C-terminal peptide of MeCP2, we found to our surprise that MeCP2 is clearly detected by immuno-staining in all glial cell types including astrocytes, oligodendrocyte progenitor cells (OPCs), and oligodendrocytes (Fig. 1a), based on co-staining for the cell-specific markers, glial fibrillary acidic protein (GFAP), NG2, and myelin basic protein (MBP), respectively. It is also expressed in microglia (not shown). Quantitative RT-PCR and Western blot analyses show that, like in neurons, *MeCP2* mRNA and protein are present in all glia (Fig. 1b–c), in astrocytes at somewhat lower levels than other glial types (Fig. 1a–c). The relative levels of MeCP2 in glia compared to neurons depend on the type of neurons;

while MeCP2 levels in glia and cerebellar granule neurons are comparable (Fig. 1c), the levels in cortical or hippocampal neurons are significantly higher (Supplementary Fig. S1a). The lack of the neuronal marker Neurofilment-L (Supplementary Fig. S1a) indicates that the presence of MeCP2 in the different glial cultures is not due to contamination with neurons in the cultures. MeCP2 in the glial cultures is not an artifact of the enrichment process either, because acutely dissociated cerebellar cultures [Post-natal day 8 (P8)] containing both glia and neurons also showed clear glial-MeCP2 immunostaining (Supplementary Fig. S2).

To determine whether MeCP2 is present in adult glia, protein was isolated from optic nerves, which contain glial, but not neuronal cell bodies. Western blot analysis revealed that MeCP2 is abundant in early post-natal as well as in adult optic nerve (Fig. 1c, right panel). Importantly, immunostaining of brain sections for MeCP2 and cell-specific markers (Fig. 1d and data not shown) indicated that, in addition to optic nerve, MeCP2 was detected in nuclei of astrocytes, OPCs, and oligodendrocytes of adult rat and mouse cerebral cortex. Together, our data clearly indicate that MeCP2 is present not only in neurons, but also in all types of glia in post-natal brain.

The discrepancy between previous published studies [17,21,28] and our studies is likely due to the presence of high levels of MeCP2 in cortical neurons and the relatively low levels in glia, and the efficiency of anti-MeCP2 antibodies used. When using a commercially available antibody, MeCP2 indeed can be detected in cortical neurons but not in glia (Supplementary Fig. S3a). However, using an efficient antibody and/or Biotin/Strepavidin enhancement system, MeCP2 can be detected in both, neuronal and astrocytic nuclei, although MeCP2 levels in the cortical neurons, are higher than in astrocytes (Supplementary Fig. S3b–d).

RTT astrocytes cannot support normal neuronal growth

Because MeCP2 is present in glia of normal brains, we reasoned that the lack of functional MeCP2 in glia of RTT brains might influence neuronal properties in a non-cell-autonomous fashion. We focused on astrocytes, the most abundant non-neuronal cells in the central nervous system, which play central roles in neurodegenerative processes [29]. We first examined whether MeCP2 was absent in astrocytes of RTT mouse brains. Co-immunostaining for MeCP2 and GFAP on brain sections showed, that while MeCP2 is present in astrocytes of normal brains, it was clearly absent in astrocytes of RTT brains (Fig. 2a). Furthermore, Western blot analysis of protein extracts from primary cultures of astrocytes, isolated from post-natal brains, showed high levels of MeCP2 in wild-type astrocytes and lack of MeCP2 in RTT astrocytes (Fig. 2b and Supplementary Fig. S1b). The presence of MeCP2 in protein extracts of the wild-type astrocyte cultures is not due to the presence of neuronal cells in the cultures as evidenced by the absence of the neuronal marker Neurofilament-L (Supplementary Fig. S1b).

Because MeCP2 recruits the histone modifying enzymes HDAC and H3K9me3 methyltransferase, which are often associated with gene repression or silencing, we asked whether MeCP2-deficient astrocytic chromatin was in a derepressed state. Histones were extracted from astrocytes of RTT and wild-type brains and analyzed by Western blotting for the presence of acetylated histone H3 and tri-methylated lysine 9 on histone H3 (H3K9me3). H3K9me3 was clearly reduced in MeCP2-null astrocytes compared to wild-type astrocytes, while acetylated histone H3 was elevated (Fig. 2c), consistent with reductions or loss of H3K9 methyltransferase and HDAC activities, respectively. Such elevated levels of acetylated histone H3 and reduced levels of tri-methylated lysine 9 on histone H3 were also found in whole RTT brains [17,30]. These data point to the importance of the presence of MeCP2 in astrocytes for maintaining proper histone modifications and suggest that the

changes in histone modifications in MeCP2-null astrocytes to a more permissive state may affect normal astrocytic functions.

To examine whether MeCP2-dysfunction in astrocytes could influence neuronal properties, we exploited a co-culture system in which neurons cultured in serum-free medium are dependent for their growth exclusively on the presence of an astrocytic feeder layer at short distances from the neurons [31,32]. Consistent with the published data, hippocampal neurons from wild-type mice died after 2–3 days in the absence of astrocytes (data not shown); in the presence of wild-type astrocytes, the neurons appeared healthy and extended long and extensive dendritic arbors as indicated by microtubule associated protein 2 (MAP2) immunostaining (Fig. 3a–b). However, wild-type hippocampal neurons co-cultured with astrocytes from RTT mice, were clearly compromised. Specifically, these neurons lacked fine processes and had fewer long processes (Fig. 3a–b). Additionally, MAP2 showed abnormal somal concentrations (Fig. 3b), likely due to the fewer and shorter dendrites. While only 5% of wild-type neurons exhibited processes shorter than 50 μm in length, up to 40% of the neurons displayed stunted dendrites of this length when co-cultured with astrocytes from RTT mice (Fig. 3c). Although neuronal densities after 3 days in culture were similar (not shown), after 6 days in the presence of astrocytes from RTT mice, densities were lower by 35% than in the presence of wild-type astrocytes (Supplementary Fig. S4a). These results suggest that, unlike wild-type astrocytes, MeCP2-null astrocytes cannot support normal neuronal growth, pointing to the significant role of functional MeCP2 in astrocytes in supporting the neurons in the brain. Importantly, using the Golgi staining method to detect dendritic arbors in brain sections from symptomatic RTT and wild-type littermates, we found aberrant neuronal morphologies in the RTT brains resembling those seen in culture (Supplementary Fig. S5). Specifically, CA3 pyramidal neurons in the hippocampus of RTT mice had fewer dendritic branches relative to wild-type CA3 pyramidal neurons (Supplementary Fig. S5a–b). Similar aberrant dendritic morphologies were observed in dentate granule neurons of RTT mice (Supplementary Fig. S5c–d). These data suggest that the abnormal neuronal morphologies in RTT brains are the result of MeCP2 dysfunction and that the aberrant morphologies seen in cultures are not an *in vitro* artifact.

RTT ACM cannot support normal neuronal growth

To examine whether the defects that occur in neurons in the co-culture system result from aberrant secretion of soluble factors by the mutant astrocytes, we generated astrocytic conditioned media (ACM). Wild-type hippocampal neurons were cultured with ACM generated either from wild-type or MeCP2-deficient astrocytes and their ability to support neuronal growth was analyzed over a 6-day-period. No differences were observed in neuronal growth and morphology over a period of 3-days in culture with either ACM (data not shown); however, at later time points, conditioned medium from MeCP2-null astrocytes elicited a robust phenotype reflected in stunted dendritic morphology (Fig. 4a, left and middle panels, compare wild-type ACM to Mut ACM) and neuronal densities were reduced by 35% (Supplementary Fig. S4b). We counted the fraction of neurons with short dendrites and found that up to 80% of the neurons showed abnormal dendritic morphology as opposed to wild-type ACM where only 10–15% of the neurons showed such aberrant morphology (Fig. 4b). Mixing the wild-type and mutant ACM in a 1:1 ratio resulted in similar dendritic defects (Fig. 4a–b), suggesting that heterozygous mutations in MeCP2 as occur in RTT patients, and which also result in mosaic expression of MeCP2 in glia likely affect the neurons similarly.

To verify that the effects of MeCP2-null astrocytes on neurons are not specific to one type of MeCP2 mutation, but rather represent a general characteristic of dysfunctional MeCP2 in astrocytes, we analyzed a mouse model that carries a different mutation in MeCP2. We first

examined the wild-type (+/y) and RTT astrocytes (−/y) of this mouse model for the presence and absence of MeCP2, respectively. Immunohistochemistry of brain sections of 6-week-old littermates showed that while MeCP2 is clearly present in the nuclei of astrocytes of wild-type brains, it is absent in astrocytes of RTT brains (Supplementary Fig. S6a). Furthermore, western blot analysis revealed that MeCP2 is absent in protein extract from MeCP2-null astrocytes while clearly present in wild-type astrocytes (Supplementary Fig. S6b). We generated conditioned media from primary cultures of astrocytes of this mouse model and analyzed their ability to support neuronal growth. Similarly to the results with the first mouse model, conditioned medium generated from MeCP2-null astrocytes was unable to support normal neuronal growth (Fig. 4c–d). Over 70% of the neurons had short dendrites compared to 20% when neurons were cultured in wild-type ACM (Fig. 4d). In this case, however, although we noticed some cell death, it was statistically insignificant (Supplementary Fig. S4c), indicating that the aberrant neuronal morphology conferred by the mutant astrocytes is independent of cell densities or survival.

To further eliminate the possibility that neuronal density may underlie the aberrant neuronal morphology by MeCP2-null astrocytes or their conditioned medium, we prepared low-density cultures of hippocampal neurons. Where individual neurons could be visualized, aberrant dendritic morphology was evident when cultured with conditioned medium from mutant but not wild-type astrocytes (Fig 5a). Thus, the inability of MeCP2-null astrocyes to support normal neuronal morphology is independent of neuronal cell densities. In addition, to visualize dendritic morphology of single neurons cultured at normal density (Fig. 4), we transfected hippocampal neurons with a GFP-expressing vector and examined the cultures 6 days after transfection (Fig. 5b). Seventy percent of the GFP-expressing neurons showed stunted processes when cultured with conditioned medium from mutant astrocytes, while only 15% showed similar morphology with wild-type conditioned medium. Therefore, the changes that we detect in neuronal morphology using MAP2 staining are reflected at the single cell level.

Finally, we asked whether MeCP2-null neurons are supported by conditioned medium generated from wild-type astrocytes. Similar to wild-type neurons, MeCP2-null neurons showed aberrant dendritic morphology when cultured with conditioned medium from MeCP2-null astrocytes (Fig. 4e); however, when cultured with wild-type ACM, they appeared healthy with normal dendritic morphology (Fig. 4e). Furthermore, while 70% of the MeCP2-null neurons had short dendrites when cultured in mutant ACM, only 10% of the neurons had short dendrites when cultured with conditioned medium from wild-type astrocytes (Fig. 4f). Together, these results suggest that MeCP2-dysfunction in glia likely contribute to the abnormal dendritic morphology of neurons in a non-cell autonomous fashion.

Discussion

Increasing evidence supports the idea that glia of all types, including astrocytes, oligodendrocytes, and microglia, each of which has close contact with neurons, help support, in various ways, the neighboring neurons. For example, astrocytes, the major cellular component of the central nervous system (CNS), play important roles in synapse formation and plasticity, and in preventing neuronal excitotoxicity by rapid removal of excess glutamate through glutamate transporters [33,34]. Thus, it is perhaps not surprising that many neurodegenerative diseases, including amyotrophic lateral sclerosis (ALS), spinocerebellar ataxia (SCA), Huntington’s disease, Parkinson’s disease and multiple system atrophy (MSA), were recently shown to have an astrocytic component. In these disorders, mutant products in astrocytes and microglia damage neighboring neurons, either by release of toxic components or by mutant-mediated reduction in neuronal support functions [29].

Astrocytes can also affect neurons indirectly. For example, multiple sclerosis (MS), which is caused by oligodendrocyte degeneration, is initiated and progressed in part by astrocytes expressing toxic compounds, which then damage oligodendrocytes, leading to impaired neuronal signaling [35,36].

RTT is distinguished from these other neurodegenerative or neurological disorders in being initiated by loss of MeCP2 function rather than by gain of function of a toxic mutant protein. While previous studies focused on MeCP2 loss-of-function in brain and specifically in neurons, the effects in non-neuronal cells in the brain were generally overlooked. Earlier in vivo experiments, however, suggested that further studies were warranted: (i) Gene expression profiles of postmortem female RTT brain revealed decreased levels of expression of neuronal genes encoding synaptic markers and increased levels of expression of glial genes involved in neuropathological mechanisms [37], and (ii) MRI and MRS studies showed that not only neuronal but also glial metabolism was affected in RTT mouse brain [38,39]. Despite these changes, obvious neuronal and glial degeneration had not been reported in Rett Syndrome [40], and the balance between neuronal and glial lineages produced from neural progenitors appeared normal [21]. Further, the amounts of GFAP in different regions of wild-type and RTT brains, as well as in astrocytic cultures from RTT and wild-type mice, are indistinguishable from each other (Supplementary Fig. S1 and data not shown), indicating that the number of astrocytes in RTT and wild-type brains is similar. These observations suggest that Rett Syndrome is not caused by reduced numbers but rather by dysfunction of specific cell types in the brain. Nonetheless, unlike mutant neurons, studies addressing the direct involvement of mutant glia in the neuropathology of Rett Syndrome have been lacking, in part due to the uncertainty of the presence of MeCP2 in glia.

Our studies show that MeCP2 is expressed not only in neurons, but also in all types of glia of normal adult brain, while it is absent in glia of RTT brain. Importantly, our co-culture studies show that astrocytes from RTT male mice, as well as their conditioned medium, cause aberrant dendritic morphology in both mutant and wild-type neurons, which resemble hippocampal pyramidal and granule cell abnormalities in conventional RTT male animals *in vivo*. This suggests that, in female human Rett Syndrome patients, who are mosaic for loss of MeCP2 function, wild-type neurons are likely to be affected in a non-cell autonomous fashion by the mutant astrocytes. Supporting this notion is the finding that in heterozygous human patients, the majority of pyramidal cortical neurons show aberrant dendritic morphology [41]. Furthermore, in culture, both RTT and wild-type neurons survive and extend processes in the presence of conditioned medium from wild-type, but not mutant astrocytes. This observation suggests that, consistent with *in vivo* studies, the damage to mutant neurons is not irreversible [20] and thus potentially can be rescued by therapeutic intervention.

While aberrant dendritic morphology was the predominant effect of MeCP2-null astrocytes on the neurons, at least to some extent, neuronal survival was also affected. Although it is generally accepted that Rett Syndrome is not a neurodegenerative disorder, several earlier studies suggest that some neurodegeneration occurs in human RTT [42,43]. Further studies are required to address more systematically whether mild neuronal degeneration occurs, at least in some circumstances, in RTT patients.

The astrocytic effect could be due to depletion of a molecule essential for neuronal dendritic morphology or to a soluble secreted factor that is detrimental to neurons. For example, depletion of neurotrophic factors such as the glial-cell-line-derived neurotrophic factor, GDNF, which affects dendritic branching, or molecules secreted from glia with deleterious effects such as tumor necrosis factor-alpha (TNFα) and nitric oxide (NO), could cause aberrant morphology and/or loss in neuronal functions. By screening for several gene candidates whose aberrant expression could potentially perturb the levels of such essential

molecules, we found that the expression of the branched-chain aminotransferase (BCAT) mRNA was up-regulated by 3-fold in MeCP2-null relative to wild-type astrocytic cultures. BCAT catalyzes the transamination of branched chain amino acids, the nitrogen donor for synthesis of glutamate in the brain, and thus can modulate the supply of glutamate. Further biochemical studies will determine whether a toxic factor is secreted from the mutant astrocytes. In this case, identification of the aberrantly secreted factor(s) could ultimately provide a means of pharmacological intervention for RTT.

Astrocytes in RTT animals could damage neurons through different non-cell autonomous pathways. It could be that: (i) astrocytes are not affected directly by loss of MeCP2 function, but the mutant neurons stimulate damaging responses from glia that then affect the neurons; (ii) astrocytes are affected directly by loss of MeCP2 and this is the primary source of neurotoxicity; (iii) both astrocytes and neurons are affected directly by loss of MeCP2, but loss of MeCP2 from glia causes a glial damage response that enhances the initial damage in neurons. The later scenario has precedence in ALS; although mutant SOD1 expression in motor neurons is required for disease initiation, neurotoxicity is additionally produced by damage within the neighboring mutant glia, which facilitates the initiation and progression of the disease [44,45]. Further *in vivo* studies are required to distinguish between these possible mechanisms. Towards this end, we are currently generating mouse models in which MeCP2 null astrocytes are produced in a background of wild type neurons. Preliminary findings suggest that loss of MeCP2 selectively in astrocytes elicits, at least in part, a RTT-like phenotype, including decreased body weight and hindlimb clasping, supporting the notion that MeCP2-dysfunction in glia contributes to the neuropathology of Rett Syndrome.

Methods

All animal studies were approved by The Institutional Animal Care and Use Committee at Stony Brook University and OHSU.

Primary cultures of rat glia

Rat glial cultures were prepared from cortices of P1–P2 pups using the differential adhesion method [46,47]. Cerebral cortices were digested in S-MEM (Gibco) containing 0.1% trypsin (Worthington), and triturated with 60 μg/ml DNase I (Sigma) and 10% FBS (GIBCO). Dissociated cells from 2 to 3 pups were plated in a 75cm^2 tissue culture flask coated with 100μg/ml poly-L-lysine (Sigma) in DMEM containing 10% FBS and 2mM glutamine. After 10 days, with a medium change every 3 days, flasks were sealed and shaken at 250 rpm at 37 C for 15–18 h followed by additional 30 min at 350 rpm. Adherent cells (astrocytes) were dissociated with 0.1% trypsin and passaged using the same medium. Detached cells were collected and plated on tissue culture dishes for 30 min at 37°C to eliminate contaminating astrocytes and microglia. The non-adherent cells (oligodendrocyte progenitor cells (OPCs)) were collected and replated overnight in DMEM containing 10% FBS at densities between 6,000 and 8,000 cells/cm^2 in tissue culture dishes or coverslips coated with 10 μg/ml poly-L-lysine after which medium was replaced with B27/NB-A (GIBCO) medium containing 10 ng/ml PDGF AA and FGF. For oligodendrocyte differentiation, growth factors were withdrawn from the medium after 3 days and replaced with DMEM containing 0.5% FBS, N1 (GIBCO), 30 ng/ml T3 and 40 ng/ml T4 (Sigma). Under these conditions, enriched glial cultures contained > 95% GFAP-positive astrocytes, ~90% NG2-positive OPC and ~85% MBP-positive oligodendrocytes.

Culturing mouse astrocytes and preparation of ACM

Cortices from P1–P2 −/y and +/y littermates were dissociated in S-MEM medium (GIBCO) containing 20 U/ml Papain (Worthington), 0.25 mg/ml L-cysteine, and 40 μg/ml DNase

(Sigma). Papain was inactivated with L15 medium containing 50 μg/ml BSA, 40 μg/ml DNase, and 1 mg/ml soybean trypsin inhibitor (Sigma). Cortices were triturated and plated on 100 μg/ml poly-L-lysine coated 25 cm^2 tissue culture flasks, in DMEM medium containing 10% FBS (GIBCO) and 2mM glutamine. When confluent (after 6–7 days), astrocytes were dissociated with TrypLE (GIBCO) and passaged to a 10 cm poly-L-lysine coated flask. Astrocyte conditioned media were prepared essentially as described (Misonou and Trimmer, 2005). Briefly, astrocytes were plated in the second passage onto poly-L-lysine-coated 10 cm tissue culture dishes. When cultures were > 95% confluent, the medium was completely replaced with serum free neuronal maintenance medium as described. Over 95% of the cells were GFAP-positive in both −/y and +/y cultures. “Conditioned” neuronal maintenance media were collected at 7 and 14 days, combined, centrifuged at 1000 × *g* for 5 min, filtered, aliquot, and stored at −80C.

Hippocampal neuron: astrocyte co-cultures

Unless otherwise stated, all the co-culture experiments were performed with astrocytes and neurons isolated from the Jaenisch MeCP2-knockout mice. Hippocampi from P1 −/y and +/y littermates were dissociated with Papain as described above for mouse astrocytes. The co-culture of the neurons with astrocytes was performed as described [32]. Hippocampal neurons (80,000 standard density) in neuronal plating medium were plated onto each coverslip containing paraffin dots and coated with 0.5 mg/ml poly-L-lysine [32]. When neurons adhered (after 3–4 hours), medium was discarded and coverslips were inverted and placed in a 12-well-dish containing a monolayer of astrocytes (50–60% confluence) in a serum-free neuronal maintenance medium [32]. Cytosine arabinoside (2 μM) was added three days after plating to limit glial proliferation. For culturing hippocampal neurons in ACM, neurons were plated on coverslips as described above at standard density or low density (40,000), but without paraffin dots. After neurons adhered, neuronal plating medium was replaced with 1 ml of a 1:1 mixture of ACM and neuronal maintenance medium. Cytosine arabinoside was added as described above.

Transfection of hippocampal neurons with GFP expression vector

Hippocampal neurons cultured in ACM (3 DIV) were transfected with *pmaxCloning* vector (Amaxa) containing GFP coding sequences under the control of the CMV promoter, as follows: 4 μl Lipofectamine 2000 (Invitrogen) was incubated in 100 μl MEM (GIBCO) for 5 min at room temperature and added to an equal volume of MEM containing 0.1 μg of DNA. Following 30 min incubation at room temperature, the DNA/Lipofectamine mix was added to the neurons, after removal of the ACM, for 90 min at 37°C, after which it was replaced with fresh ACM. After 24 hours, GFP was visible in approximately 0.1% of the neurons.

RNA Isolation, and Quantitative Real-Time RT-PCR analysis

Total RNA was prepared from cells using RNeasy (Qiagen), and treated with RNase-free DNase (Ambion, DNA-free kit). For reverse transcription, First Strand Superscript II (Invitrogen) was used and quantitative real-time PCR was performed in an ABI PRISM 7700 Sequence Detector using SYBR-green PCR master mix (PE Applied Biosystem). Relative abundance of the specific mRNAs was normalized to *GAPDH* mRNA. The primer sets used for quantitative real-time RT-PCR are as follows: *MeCP2*, forward 5′-AAG AGG GCA AAC ATG AAC CAC T -3′, reverse 5′-TTG CCT GCC TCT GCT GG -3′; *GAPDH*, forward 5′-AAG TAT GAT GAC ATC AAG AAG GTG GT-3′, reverse 5′-AGC CCA GGA TGC CCT TTA GT-3′.

Immunocytochemistry

Cells were fixed with 4% paraformaldehyde and probed with rabbit anti-MeCP2 (a generous gift from Dr. M. Greenberg, Harvard Medical School, Boston), mouse anti-MAP2 (Chemicon), mouse anti-MBP (Chemicon), mouse anti-GFAP (Chemicon), or mouse anti-neuronal β-tubulin (TUJ1, Chemicon), followed by incubation with the appropriate secondary antibody conjugated to Alexa Fluor (Molecular Probes) [48]. For NG2 staining, mouse anti-NG2 (a generous gift from Dr. J. Levine, Stony Brook University, NY) in L15 medium was applied to living cells for 45 min after which cells were washed and fixed as above. In this case, a second primary antibody was applied sequentially after fixation and cells were probed with secondary antibodies described above. Images were collected on a Zeiss confocal laser scanning LSM 510 microscope.

Immunohistochemistry

Mice or rats were transcadially perfused with PBS-buffered 4% paraformaldehyde. Brains were cryoprotected overnight in 30% sucrose and coronal sections were cut (40 μm) on a freezing microtome (Bright Instruments). Sections were immunostained using the following primary antibodies: anti-MeCP2 and anti-GFAP as described above, mouse anti-RIP (Chemicon), guinea pig anti-NG2 (a generous gift from Dr. Stallcup, The Burnham Institute, La Jolla, Ca), mouse anti-NeuN (Chemicon), followed by incubation with secondary antibodies conjugated to Cyanine (Jackson ImmunoResearch). MeCP2 immunostaining was enhanced using the biotin-streptavidin conjugated secondary antibodies. Images were collected on a Zeiss confocal laser scanning LSM 510 microscope.

Whole cell protein extraction, histone extraction, and Western Blot Analysis

Nuclear and cytoplasmic cell extracts were prepared by the modified Dignam method [49]. For whole cell extracts, cells were lysed directly in nuclear lysis buffer. Histone extraction was performed using the acid extraction method [50]. The following antibodies were used for Western blot analysis: Anti-MeCP2 and anti-Sin3A, as described above, mouse anti-Neurofilament-L (Cell Signaling), mouse anti-α–tubulin (Sigma), rabbit anti-trimethyl-histone H3 lysine 9 and rabbit anti-acetyl histone H3 (Upstate), rabbit anti-histone H3 (Abcam).

Supplementary Material

Refer to Web version on PubMed Central for supplementary material.

Acknowledgments

The authors thank Dr. Joel Levine and Lisa Evans for providing the enriched glial cultures for the initial immunostaining analysis, Drs. Paul Brehm, Richard Goodman, Thomas Reese, and Gary Banker for valuable discussions about the results, and Diane D. Lu and Roman Spektor for technical assistance. The work was supported in part by a grant from the RSRF to N.B. and an NIH grant to G.M. and N.B. Gail Mandel is an Investigator of the Howard Hughes Medical Institute.

References

1. Amir RE, et al. Rett syndrome is caused by mutations in X-linked MECP2, encoding methyl-CpG-binding protein 2. Nat Genet. 1999; 23:185–8. [PubMed: 10508514]
2. Chahrour M, Zoghbi HY. The story of Rett syndrome: from clinic to neurobiology. Neuron. 2007; 56:422–37. [PubMed: 17988628]
3. Chandler SP, Guschin D, Landsberger N, Wolffe AP. The methyl-CpG binding transcriptional repressor MeCP2 stably associates with nucleosomal DNA. Biochemistry. 1999; 38:7008–18. [PubMed: 10353812]

4. Kriaucionis S, Bird A. DNA methylation and Rett syndrome. Hum Mol Genet. 2003; 12(Spec No 2):R221–7. [PubMed: 12928486]
5. Harikrishnan KN, et al. Brahma links the SWI/SNF chromatin-remodeling complex with MeCP2-dependent transcriptional silencing. Nat Genet. 2005; 37:254–64. [PubMed: 15696166]
6. Jones PL, et al. Methylated DNA and MeCP2 recruit histone deacetylase to repress transcription. Nat Genet. 1998; 19:187–91. [PubMed: 9620779]
7. Nan X, et al. Transcriptional repression by the methyl-CpG-binding protein MeCP2 involves a histone deacetylase complex. Nature. 1998; 393:386–9. [PubMed: 9620804]
8. Fuks F, et al. The methyl-CpG-binding protein MeCP2 links DNA methylation to histone methylation. J Biol Chem. 2003; 278:4035–40. [PubMed: 12427740]
9. Chen WG, et al. Derepression of BDNF transcription involves calcium-dependent phosphorylation of MeCP2. Science. 2003; 302:885–9. [PubMed: 14593183]
10. Martinowich K, et al. DNA methylation-related chromatin remodeling in activity-dependent BDNF gene regulation. Science. 2003; 302:890–3. [PubMed: 14593184]
11. Zhou Z, et al. Brain-specific phosphorylation of MeCP2 regulates activity-dependent Bdnf transcription, dendritic growth, and spine maturation. Neuron. 2006; 52:255–69. [PubMed: 17046689]
12. Yasui DH, et al. Integrated epigenomic analyses of neuronal MeCP2 reveal a role for long-range interaction with active genes. Proc Natl Acad Sci U S A. 2007; 104:19416–21. [PubMed: 18042715]
13. Chahrour M, et al. MeCP2, a key contributor to neurological disease, activates and represses transcription. Science. 2008; 320:1224–9. [PubMed: 18511691]
14. Young JI, et al. Regulation of RNA splicing by the methylation-dependent transcriptional repressor methyl-CpG binding protein 2. Proc Natl Acad Sci U S A. 2005; 102:17551–8. [PubMed: 16251272]
15. Chen RZ, Akbarian S, Tudor M, Jaenisch R. Deficiency of methyl-CpG binding protein-2 in CNS neurons results in a Rett-like phenotype in mice. Nat Genet. 2001; 27:327–31. [PubMed: 11242118]
16. Guy J, Hendrich B, Holmes M, Martin JE, Bird A. A mouse Mecp2-null mutation causes neurological symptoms that mimic Rett syndrome. Nat Genet. 2001; 27:322–6. [PubMed: 11242117]
17. Shahbazian M, et al. Mice with truncated MeCP2 recapitulate many Rett syndrome features and display hyperacetylation of histone H3. Neuron. 2002; 35:243–54. [PubMed: 12160743]
18. Gemelli T, et al. Postnatal loss of methyl-CpG binding protein 2 in the forebrain is sufficient to mediate behavioral aspects of Rett syndrome in mice. Biol Psychiatry. 2006; 59:468–76. [PubMed: 16199017]
19. Giacometti E, Luikenhuis S, Beard C, Jaenisch R. Partial rescue of MeCP2 deficiency by postnatal activation of MeCP2. Proc Natl Acad Sci U S A. 2007; 104:1931–6. [PubMed: 17267601]
20. Guy J, Gan J, Selfridge J, Cobb S, Bird A. Reversal of neurological defects in a mouse model of Rett syndrome. Science. 2007; 315:1143–7. [PubMed: 17289941]
21. Kishi N, Macklis JD. MECP2 is progressively expressed in post-migratory neurons and is involved in neuronal maturation rather than cell fate decisions. Mol Cell Neurosci. 2004; 27:306–21. [PubMed: 15519245]
22. Armstrong DD. Neuropathology of Rett syndrome. J Child Neurol. 2005; 20:747–53. [PubMed: 16225830]
23. Belichenko PV, Oldfors A, Hagberg B, Dahlstrom A. Rett syndrome: 3-D confocal microscopy of cortical pyramidal dendrites and afferents. Neuroreport. 1994; 5:1509–13. [PubMed: 7948850]
24. Moretti P, et al. Learning and memory and synaptic plasticity are impaired in a mouse model of Rett syndrome. J Neurosci. 2006; 26:319–27. [PubMed: 16399702]
25. Asaka Y, Jugloff DG, Zhang L, Eubanks JH, Fitzsimonds RM. Hippocampal synaptic plasticity is impaired in the Mecp2-null mouse model of Rett syndrome. Neurobiol Dis. 2006; 21:217–27. [PubMed: 16087343]

26. Chao HT, Zoghbi HY, Rosenmund C. MeCP2 controls excitatory synaptic strength by regulating glutamatergic synapse number. Neuron. 2007; 56:58–65. [PubMed: 17920015]
27. Dani VS, et al. Reduced cortical activity due to a shift in the balance between excitation and inhibition in a mouse model of Rett syndrome. Proc Natl Acad Sci U S A. 2005; 102:12560–5. [PubMed: 16116096]
28. Jung BP, et al. The expression of methyl CpG binding factor MeCP2 correlates with cellular differentiation in the developing rat brain and in cultured cells. J Neurobiol. 2003; 55:86–96. [PubMed: 12605461]
29. Lobsiger CS, Cleveland DW. Glial cells as intrinsic components of non-cell-autonomous neurodegenerative disease. Nat Neurosci. 2007; 10:1355–60. [PubMed: 17965655]
30. Thatcher KN, LaSalle JM. Dynamic changes in Histone H3 lysine 9 acetylation localization patterns during neuronal maturation require MeCP2. Epigenetics. 2006; 1:24–31. [PubMed: 17464364]
31. Banker GA. Trophic interactions between astroglial cells and hippocampal neurons in culture. Science. 1980; 209:809–10. [PubMed: 7403847]
32. Kaech S, Banker G. Culturing hippocampal neurons. Nat Protoc. 2006; 1:2406–15. [PubMed: 17406484]
33. Ullian EM, Sapperstein SK, Christopherson KS, Barres BA. Control of synapse number by glia. Science. 2001; 291:657–61. [PubMed: 11158678]
34. Maragakis NJ, Rothstein JD. Glutamate transporters in neurologic disease. Arch Neurol. 2001; 58:365–70. [PubMed: 11255439]
35. Antony JM, et al. Human endogenous retrovirus glycoprotein-mediated induction of redox reactants causes oligodendrocyte death and demyelination. Nat Neurosci. 2004; 7:1088–95. [PubMed: 15452578]
36. Back SA, et al. Hyaluronan accumulates in demyelinated lesions and inhibits oligodendrocyte progenitor maturation. Nat Med. 2005; 11:966–72. [PubMed: 16086023]
37. Colantuoni C, et al. Gene expression profiling in postmortem Rett Syndrome brain: differential gene expression and patient classification. Neurobiol Dis. 2001; 8:847–65. [PubMed: 11592853]
38. Saywell V, et al. Brain magnetic resonance study of Mecp2 deletion effects on anatomy and metabolism. Biochem Biophys Res Commun. 2006; 340:776–83. [PubMed: 16380085]
39. Viola A, Saywell V, Villard L, Cozzone PJ, Lutz NW. Metabolic fingerprints of altered brain growth, osmoregulation and neurotransmission in a Rett syndrome model. PLoS ONE. 2007; 2:e157. [PubMed: 17237885]
40. Jellinger K, Armstrong D, Zoghbi HY, Percy AK. Neuropathology of Rett syndrome. Acta Neuropathol. 1988; 76:142–58. [PubMed: 2900587]
41. Armstrong D, Dunn JK, Antalffy B, Trivedi R. Selective dendritic alterations in the cortex of Rett syndrome. J Neuropathol Exp Neurol. 1995; 54:195–201. [PubMed: 7876888]
42. Hanefeld F, et al. Cerebral proton magnetic resonance spectroscopy in Rett syndrome. Neuropediatrics. 1995; 26:126–7. [PubMed: 7566451]
43. Kitt CA, Wilcox BJ. Preliminary evidence for neurodegenerative changes in the substantia nigra of Rett syndrome. Neuropediatrics. 1995; 26:114–8. [PubMed: 7566448]
44. Clement AM, et al. Wild-type nonneuronal cells extend survival of SOD1 mutant motor neurons in ALS mice. Science. 2003; 302:113–7. [PubMed: 14526083]
45. Yamanaka K, et al. Mutant SOD1 in cell types other than motor neurons and oligodendrocytes accelerates onset of disease in ALS mice. Proc Natl Acad Sci U S A. 2008; 105:7594–9. [PubMed: 18492803]
46. McCarthy KD, de Vellis J. Preparation of separate astroglial and oligodendroglial cell cultures from rat cerebral tissue. J Cell Biol. 1980; 85:890–902. [PubMed: 6248568]
47. Yang Z, Watanabe M, Nishiyama A. Optimization of oligodendrocyte progenitor cell culture method for enhanced survival. J Neurosci Methods. 2005; 149:50–6. [PubMed: 15975663]
48. Ballas N, et al. Regulation of neuronal traits by a novel transcriptional complex. Neuron. 2001; 31:353–65. [PubMed: 11516394]

49. Grimes JA, et al. The Co-repressor mSin3A Is a Functional Component of the REST-CoREST Repressor Complex. J Biol Chem. 2000; 275:9461–9467. [PubMed: 10734093]

50. Shechter D, Dormann HL, Allis CD, Hake SB. Extraction, purification and analysis of histones. Nat Protoc. 2007; 2:1445–57. [PubMed: 17545981]

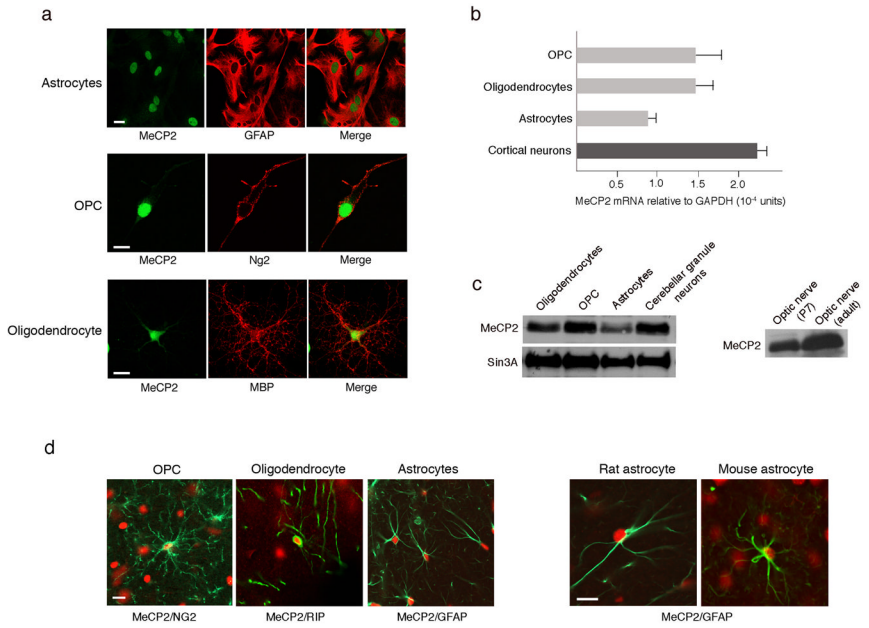

Figure 1. MeCP2 is present in all glial cell types in normal rat and mouse brains

(a) Immunostaining showing MeCP2 is present in nuclei of cultured rat glia. MeCP2 protein (green) and cell-specific marker proteins (red) are indicated. Calibration bar, 20 μm. (b) Real time RT-PCR analysis showing MeCP2 mRNA levels in rat glia. MeCP2 transcripts in cortical neurons are shown for comparison. Error bars represent standard deviation (SD) based on three independent experiments. (c) Western blot analysis showing MeCP2 protein in rat glia (left panel) and optic nerve (right panel). MeCP2 and Sin3A migrate at 75 kDa and 150kDa, respectively. (d) Co-immunostaining of rat or mouse brain sections for MeCP2 (red) and the glial-specific markers (green) as indicated. Calibration bars, 20 μm.

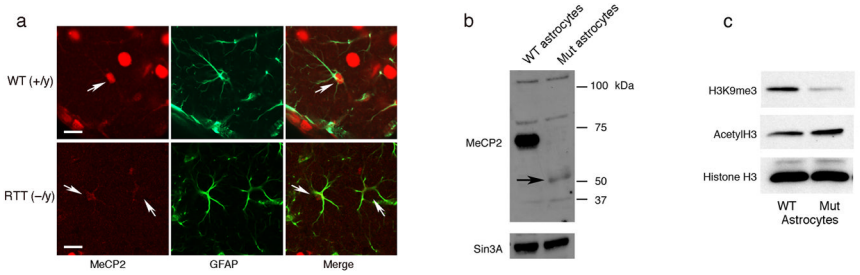

Figure 2. MeCP2 is detected in astrocytes in brain sections from wild-type but not MeCP2-null mice

(a) Co-immunostaining of brain sections from 6-week-old wild-type (+/y) and RTT (−/y) mice for MeCP2 (red) and GFAP (green). Arrows indicate the presence and absence of MeCP2 in astrocyte nuclei of wild-type (WT) and RTT brains, respectively. Calibration bars, 40 μm. (b) Western blot analysis confirms the presence of MeCP2 in WT and its absence in MeCP2-null astrocytes. Arrow indicates MeCP2 C-terminal peptide product of the recombination event in the Jaenisch mouse model. Sin3A serves as loading control. (c) Western blot showing an altered global chromatin signature in astrocytes from RTT mice (Mut). Histones were probed with the indicated antibodies to histone modifications.

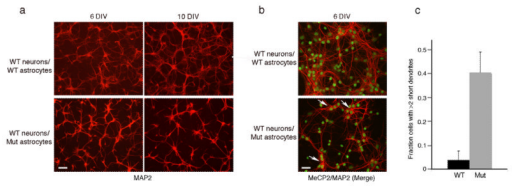

Figure 3. Wild-type hippocampal neurons co-cultured with cortical astrocytes from RTT mice exhibit stunted dendrites

(a) Aberrant morphology of hippocampal neurons, visualized by MAP staining (red), increases with time in culture. Wild-type (WT) hippocampal neurons co-cultured with either WT astrocytes (top panels) or Mutant (Mut) astrocytes (bottom panels). Note the decrease in fine processes and their shorter length of processes when co-cultured with mutant astrocytes. Calibration bar, 100 μm. (b) Immunostaining for nuclear MeCP2 (green) and MAP2 (red) showing the aberrant cytoplasmic MAP distribution (arrows) in WT hippocampal neurons cultured with Mut astrocytes. Calibration bar, 40 μm. DIV, Days In Vitro. (c) Bar graphs represent the fraction of neurons with at least two short (<50 μm) dendrites when co-cultured with WT or Mut astrocytes. Error bars represent SD based on three independent experiments.

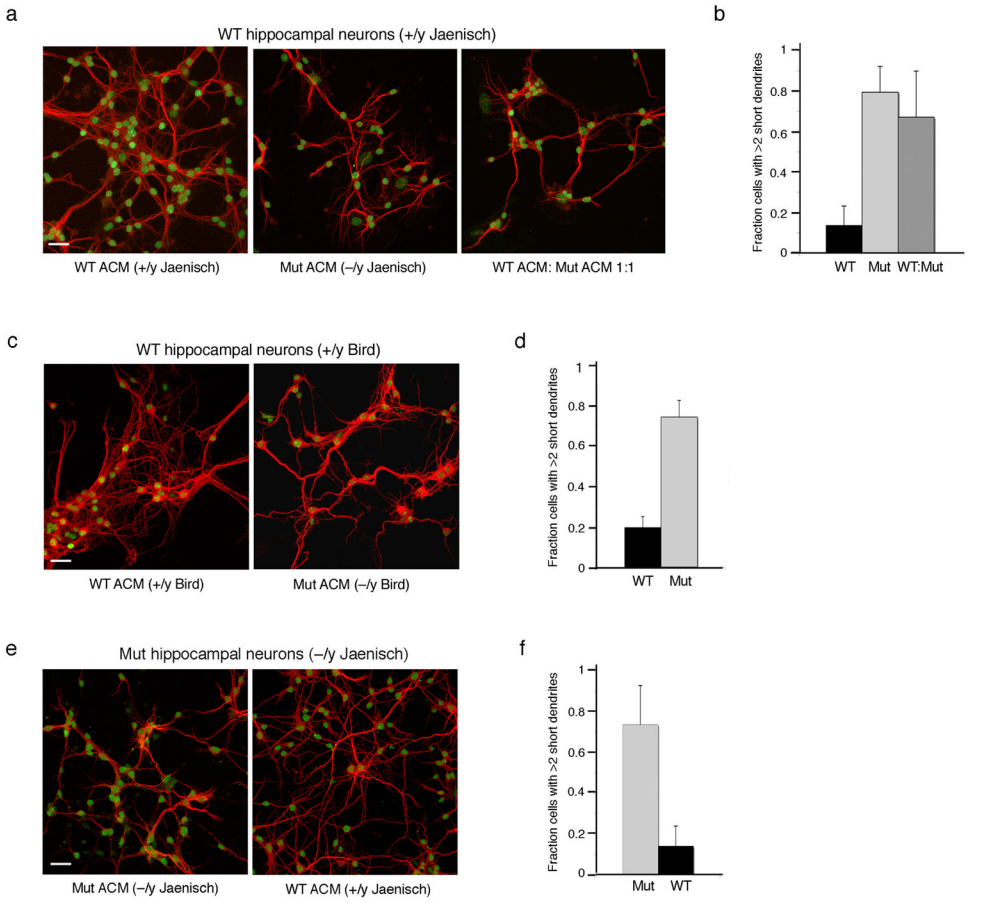

Figure 4. Conditioned medium from MeCP2-null astrocytes cannot support normal neuronal growth

Co-immunostaining of hippocampal neurons with MAP2 as dendritic marker (red) and MeCP2 (green). (a) Hippocampal neurons from WT mice cultured for 6 days in astrocytic conditioned media (ACM) from wild-type (WT), MeCP2-null astrocytes (Mut), or with mixed ACM from WT and mutant astrocytes. (b) Bar graphs represent the fraction of neurons with at least two short (>50 mm) dendrites when cultured in the different ACM. Error bars represent SD based on three independent experiments. (c) WT hippocampal neurons cultured for 7 days with conditioned medium generated from MeCP2-null astrocytes of the Bird mouse model show similar abnormal morphology. (d) Bar graphs as in b. (e) Hippocampal neurons from RTT mice (Mut) cultured for 6 days are supported by conditioned medium from WT astrocytes (WT ACM). (f) Bar graphs as in b. Note that the gain of image in Mut hippocampal neurons is increased for MeCP2 because MeCP2-null neurons from the Jaenisch mouse model express low levels of the C-terminus, which is recognized by the anti-MeCP2 antibody used. Calibration bars, 40 μm.

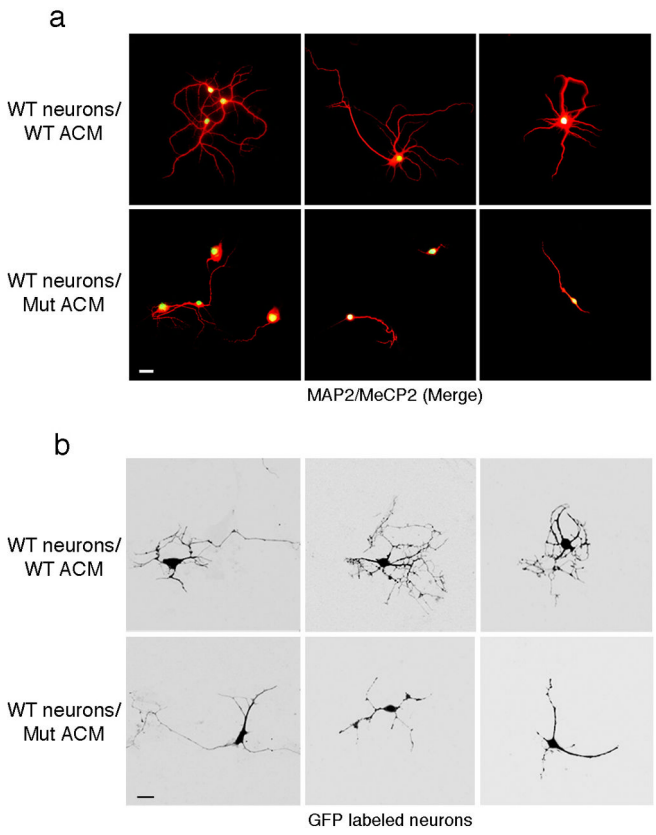

Figure 5. Altered morphology of wild-type neurons cultured with ACM from MeCP2-null astrocytes is evident at the single cell level

(a) Co-immunostaining in low-density neuronal cultures (6 DIV) with MAP2 (red) and MeCP2 (green) demonstrating aberrant process morphology when cultured in ACM from mutant astrocytes (compare top panels, WT ACM to lower panels Mut ACM). Calibration bar, 30 μm. (b) GFP-expressing neurons show aberrant processes when cultured in mutant ACM (compare top panels, WT ACM to lower panels Mut ACM). Calibration bars, 20 μm.